

Thermal expansion of MgSiO₃ and FeSiO₃ ortho- and clinopyroxenes

DEMELZA HUGH-JONES

Department of Earth Sciences, University of Cambridge, Downing Street,
Cambridge CB2 3EQ, U.K.

ABSTRACT

Unit-cell parameters of synthetic (Mg,Fe)SiO₃ ortho- and clinopyroxenes were determined at regular intervals in the temperature range 293–1094 K using powder X-ray diffraction techniques. Volume thermal expansion coefficients calculated from these data show that orthopyroxenes expand faster than clinopyroxenes (i.e., $\alpha_{\text{opx}} > \alpha_{\text{cpx}}$), irrespective of their composition along the MgSiO₃-FeSiO₃ join. For both ortho- and clinopyroxenes, α_{MgSiO_3} exceeds α_{FeSiO_3} . Axial thermal expansion coefficients calculated for each of the pyroxene phases studied here are a complex function of the changes in structure at high temperature. Thermodynamic calculations of the position of the phase boundary between MgSiO₃ ortho- and clinopyroxene show excellent agreement with the experimentally reversed boundary.

INTRODUCTION

Ca-poor pyroxenes are important components of the Earth's upper mantle, being stable to depths of ~400 km where they transform to higher density garnet structures (e.g., Gasparik 1990). The phase diagram of MgSiO₃ pyroxene has been characterized by Pacalo and Gasparik (1990) and Angel and Hugh-Jones (1994), and that of FeSiO₃ pyroxene by Hugh-Jones et al. (1994). The topologies of these two phase diagrams are almost identical [the triple point in the FeSiO₃ system is simply shifted to somewhat lower pressures than that for MgSiO₃ (Angel et al. 1994)], with clinopyroxene (with space group *P2₁/c*) being stable at ambient temperatures and pressures, and the stability field of orthopyroxene (space group *Pbca*) being at higher temperatures than this. Metastable Ca-poor orthopyroxene is also commonly found at ambient conditions (e.g., see Smith 1969).

Although the behavior of (Mg,Fe)SiO₃ ortho- and clinopyroxenes at high pressures was recently characterized in some detail (Hugh-Jones and Angel 1994; Hugh-Jones et al. 1994), relatively little is known about their response to high temperatures. There have been a few measurements of the thermal expansivity of such Ca-poor ortho- and clinopyroxenes, but the relative thermal expansion of the two phases is essentially unknown. For example, whereas Skinner (1966) suggested that, at room temperature, the volume thermal expansion coefficient, α_v , of MgSiO₃ orthoenstatite slightly exceeds that of clinoenstatite, Sarver and Hummel (1962) reported thermal expansion coefficients for the same materials with the relative expansivities reversed. More recent studies have not compared the relative expansivities of the two polymorphs, but report, for example, values for the volume thermal expansion coefficient of MgSiO₃ orthoenstatite at room temperature in the range $20.8 \times 10^{-6} \text{ K}^{-1}$ (Dietrich and

Arndt 1982) to $47.7 \times 10^{-6} \text{ K}^{-1}$ (Frisillo and Buljan 1972), and values for Fe²⁺-rich orthopyroxene in the range $29.0 \times 10^{-6} \text{ K}^{-1}$ (Yang and Ghose 1994) to $43.8 \times 10^{-6} \text{ K}^{-1}$ (Smyth 1973). There is similar uncertainty in the values of thermal expansion coefficients of the corresponding (Mg,Fe)SiO₃ clinopyroxene phases. Such inconsistencies have serious implications for calculation of the pyroxene phase diagram at high temperatures and modest pressures; this problem is discussed in more detail below.

The object of this study was to determine which of the two pyroxene polymorphs (ortho or clino) expands more over a given temperature range and then to provide precise values of their respective thermal expansion coefficients. Synthetic samples of both the end-member phases of the (Mg,Fe)SiO₃ solid solution were used to obtain further information about the relative effects of Mg and Fe²⁺ in the cation sites of pyroxene.

EXPERIMENTAL METHODS

A large sample of MgSiO₃ orthoenstatite was synthesized from a stoichiometric mixture of MgO and SiO₂ contained within a gold capsule using a piston-cylinder apparatus. The experiment conditions were 2.0 GPa and 950 °C for 24 h. MgSiO₃ clinoenstatite was produced by heating a portion of this MgSiO₃ orthoenstatite sample in a gas-mixing furnace at 1200 °C for 18 h and then rapidly quenching it to room temperature. This temperature is within the protoenstatite stability field (Gasparik 1990), so that the clinoenstatite phase was formed directly from protoenstatite during the quench. A sample of fayalite (Fe₂SiO₄), used as a starting material in the synthesis of FeSiO₃ orthoferrosilite, was made by annealing a stoichiometric mixture of Fe₂O₃ and SiO₂ in a gas-mixing furnace at 1100 °C for 24 h at a controlled oxygen fugacity

just above the iron-wüstite buffer. Subsequent synthesis of the orthoferrosilite was achieved by treating a stoichiometric mixture of this fayalite plus SiO₂ to conditions of 950 °C and 2.0 GPa for 24 h in the piston-cylinder apparatus; the sample was contained in a gold capsule. After each of these syntheses, a small portion the product was examined using a powder diffractometer to ensure complete reaction of the starting materials and the absence of any impurities. Although the FeSiO₃ orthoferrosilite was pure within the resolution of the instrument, a small amount of quartz remained in the MgSiO₃ orthoenstatite sample (with corresponding traces of coesite in the clinoenstatite sample); this quartz proved to be an invaluable indicator of the quality of the high-temperature data obtained. The FeSiO₃ clinoferrosilite sample, kindly donated by Alan Woodland, was synthesized from a mixture of fayalite and quartz at 9 GPa and 1100 °C using the multi-anvil press at the Bayerisches Geoinstitut.

For each experiment, mixtures of equal amounts of ortho- and clinopyroxene of a given composition were used, because it was suspected that the difference in thermal expansion coefficients of the two phases could be merely of the order of the experimental uncertainties. Thus, in each case, approximately equal amounts of the orthopyroxene and clinopyroxene phases of a given composition were ground together to a powder and mixed with Si as an internal standard. This mixture was spread over the platinum heating strip in the heating powder diffractometer (known as the INEL; details of the diffractometer and PSD detector may be found in Salje et al. 1993); in the case of the FeSiO₃ samples, the sample chamber was then evacuated. The temperature was monitored by means of a thermocouple welded onto the platinum heating strip. The temperature controller was calibrated using a sample of pure quartz as a standard. High-temperature data were collected at approximately 50 K intervals between 293 and 1094 K. The diffraction signals were measured in the range 13° ≤ 2θ ≤ 115°, with the 2θ scale being calibrated at each temperature from the positions of the diffraction maxima of the internal Si standard. Care was taken to avoid transformation of the (Mg,Fe)SiO₃ samples to the high-clinopyroxene polymorph (with space group *C2/c*): In each experiment, the temperature was maintained below the temperature of the metastable low-high clinopyroxene transition [~900 K for FeSiO₃ (Prewitt et al. 1971) and ~1270 K for MgSiO₃ (Perotta and Stephenson 1965)]. The temperature for conversion of orthoferrosilite to the high-clinoferrosilite phase is considerably higher than 900 K (Sueno et al. 1976). Although some of the peaks of the possible *C2/c* phases would be closely overlapped with those of the *P2₁/c* phases held at the same temperature, there are sufficient strong peaks from the *C2/c* phases that their presence would be readily identifiable; no evidence existed of any diffraction peaks arising from *C2/c* phases in any of the X-ray diffraction patterns.

The diffraction maxima were fitted with Gaussian peaks using the DIFFRACTINEL software, which was designed for use with the INEL diffractometer. The pro-

TABLE 1. Unit-cell parameters for MgSiO₃ orthopyroxene constrained to orthorhombic symmetry

<i>T</i> (K)	<i>a</i> (Å)	<i>b</i> (Å)	<i>c</i> (Å)	Volume (Å ³)
293	18.230(5)	8.819(3)	5.174(2)	831.85(25)
322	18.226(5)	8.830(2)	5.185(2)	834.35(30)
370	18.227(6)	8.829(3)	5.184(2)	834.26(29)
419	18.227(6)	8.830(3)	5.195(2)	836.04(37)
467	18.276(5)	8.835(3)	5.189(2)	837.80(27)
515	18.271(9)	8.840(5)	5.185(2)	837.37(47)
563	18.287(6)	8.825(3)	5.194(2)	838.26(35)
612	18.282(9)	8.842(4)	5.196(3)	840.02(49)
660	18.276(8)	8.853(3)	5.194(3)	840.39(45)
708	18.290(9)	8.861(4)	5.200(3)	842.73(46)
756	18.313(11)	8.868(4)	5.197(3)	843.92(54)
805	18.306(7)	8.868(3)	5.205(2)	845.02(37)
853	18.321(8)	8.884(3)	5.207(2)	847.58(40)
901	18.312(5)	8.886(3)	5.214(2)	848.42(34)
997	18.316(7)	8.902(3)	5.217(2)	850.63(40)
1046	18.354(6)	8.905(3)	5.225(2)	854.00(34)
1094	18.357(5)	8.915(2)	5.226(2)	855.17(27)
1046*	18.358(5)	8.908(3)	5.226(2)	854.65(30)
949*	18.316(5)	8.892(2)	5.220(2)	850.19(31)
853*	18.309(7)	8.883(3)	5.215(2)	848.20(39)
756*	18.294(6)	8.875(3)	5.210(2)	845.84(36)
660*	18.285(7)	8.860(4)	5.200(1)	842.41(34)
563*	18.280(5)	8.853(3)	5.196(1)	840.84(26)
467*	18.272(6)	8.842(3)	5.188(2)	838.24(31)
370*	18.249(4)	8.832(2)	5.187(2)	836.05(26)
293*	18.253(5)	8.822(2)	5.183(2)	834.58(24)

* Collected on temperature decrease, the remaining on initial heating.

gram could not resolve multiplets with a spacing of less than about 0.1° in 2θ. Such unresolved overlapping peaks (i.e., the resulting “broad peaks”) were excluded from lattice parameter refinement. The number of such broad peaks in each diffraction pattern changed slightly with changing temperature, with the most significant number of closely overlapping peaks occurring for the MgSiO₃ experiment at temperatures in the approximate range 600–800 K.

The positions of the maxima of the fitted Gaussian peaks at each temperature were then assigned to either the ortho- or clinopyroxene polymorph, or, in addition, to quartz in the case of the MgSiO₃ experiment. (It was not possible to identify sufficient peaks from the coesite impurity to determine its unit-cell parameters because most of its diffraction maxima were of very low intensity.) Lattice parameters for each phase were refined from 25–50 peaks using a least-squares refinement technique that also constrained the symmetry of the phase. The lattice parameters of both ortho and clino phases of both MgSiO₃ and FeSiO₃ pyroxenes are presented in Tables 1–4. In both experiments, diffraction data were collected during both heating and cooling of the sample. No significant or systematic differences exist between the two sets of data. Possible mis-assignments of a few peaks to the wrong phase may be the cause of the data scatter.

Unfortunately, the quality of the data was not adequate to resolve whether there was any non-linearity in the behavior of some of the unit-cell parameters of the (Mg,Fe)SiO₃ pyroxenes at high temperatures; all the thermal expansion coefficients quoted below are therefore linear values, calculated according to the equation X_T / X_0

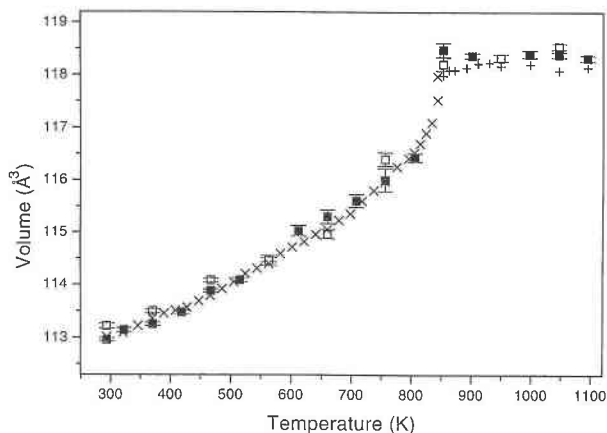


FIGURE 1. Comparison of the unit-cell volume of the quartz impurity in the MgSiO₃ experiment (squares) with the high-temperature X-ray (plus sign) and neutron (crosses) data of Graeme-Barber (in preparation). Filled squares represent data collected on increasing temperature, open squares represent those collected on cooling.

= 1 + $\alpha_x T$, where X_T represents either the unit-cell parameter b or c , the distance between (100) planes (denoted a for the orthopyroxenes and d_{100} for the clinopyroxene) or the volume of the phase at temperature T (in Kelvins), and X_0 represents the corresponding value at 293 K.

RESULTS

Quartz

Figure 1 shows the good correspondence among the values of the unit-cell volume of the quartz impurity (determined during the experiments on the sample mixture of MgSiO₃ ortho- and clinopyroxenes) and those obtained by Graeme-Barber (personal communication) during recent high-temperature X-ray and neutron experiments. The transition from low-quartz (crystal class 32) to high-quartz (crystal class 622) at 846 K is clearly observed in both sets of data. Similarly, the values of the unit-cell parameters a and c obtained from this study are within one combined estimated standard deviation (esd) of those of Graeme-Barber, each showing the characteristic change in behavior at 846 K. This agreement between the two data sets indicates that the calibration of both the 2 θ scale of the PSD detector and the temperature of the sample are correct within 0.03° and 1 K, respectively, at temperatures below 1094 K, and therefore that the unit-cell parameters of both quartz and pyroxene phases are accurate within an estimated standard deviation of less than 0.1%.

MgSiO₃

The unit-cell parameters of the ortho and clino phases of the MgSiO₃ pyroxene determined up to 1094 K are given in Tables 1 and 2. A combined plot of V/V_0 for these two phases (Fig. 2) reveals that although the re-

TABLE 2. Unit-cell parameters for MgSiO₃ clinopyroxene constrained to monoclinic symmetry

T (K)	a (Å)	b (Å)	c (Å)	β (°)	Volume (Å ³)
293	9.604(5)	8.810(4)	5.175(3)	108.35(4)	414.79(47)
322	9.607(5)	8.815(5)	5.170(4)	108.37(4)	415.53(57)
370	9.605(5)	8.819(3)	5.178(3)	108.30(4)	416.39(46)
419	9.608(5)	8.829(5)	5.186(3)	108.34(5)	417.61(47)
467	9.629(5)	8.831(5)	5.180(3)	108.42(4)	417.90(52)
515	9.626(4)	8.838(4)	5.177(4)	108.40(4)	417.92(51)
563	9.633(5)	8.848(4)	5.184(3)	108.42(4)	419.17(45)
612	9.629(9)	8.851(6)	5.199(4)	108.50(7)	420.12(67)
660	9.636(9)	8.856(6)	5.211(4)	108.64(8)	421.35(69)
708	9.638(11)	8.866(6)	5.212(6)	108.52(8)	421.48(77)
756	9.648(10)	8.874(5)	5.200(4)	108.58(13)	421.98(81)
805	9.636(8)	8.878(5)	5.185(3)	108.24(6)	421.31(61)
853	9.666(9)	8.876(7)	5.192(4)	108.46(6)	422.54(61)
901	9.651(5)	8.910(4)	5.185(4)	108.38(4)	423.11(46)
997	9.664(4)	8.913(4)	5.191(2)	108.45(3)	424.14(34)
1046	9.666(5)	8.920(5)	5.196(3)	108.38(4)	425.13(46)
1094	9.672(5)	8.928(5)	5.200(3)	108.50(4)	425.78(47)
1046*	9.670(6)	8.920(4)	5.187(4)	108.34(4)	424.69(54)
949*	9.660(6)	8.901(6)	5.192(4)	108.43(5)	423.54(54)
853*	9.652(5)	8.883(5)	5.188(2)	108.47(3)	421.90(39)
756*	9.650(5)	8.871(4)	5.186(3)	108.43(4)	421.12(47)
660*	9.644(4)	8.854(3)	5.185(2)	108.42(3)	420.04(36)
563*	9.630(4)	8.851(4)	5.186(3)	108.40(4)	419.43(44)
467*	9.631(4)	8.835(4)	5.182(3)	108.39(4)	418.42(44)
370*	9.622(4)	8.825(3)	5.177(3)	108.33(3)	417.26(40)
293*	9.617(5)	8.798(4)	5.170(3)	108.35(4)	415.19(45)

* Collected on temperature decrease, the remaining on initial heating.

sponse to temperature of the polymorphs is identical within two combined estimated standard deviations, with linear volume thermal expansion coefficients of the ortho- and clinopyroxenes being $32.2(1.1) \times 10^{-6} \text{ K}^{-1}$ and $29.9(1.1) \times 10^{-6} \text{ K}^{-1}$ respectively, the orthopyroxene phase does in fact expand noticeably more than the clinopyroxene. Note that the amount of overlap of the ortho- and clinopyroxene peaks increased significantly in the temperature range ~600–800 K, causing the somewhat increased amount of scatter in the unit-cell data at these temperatures (e.g., Fig. 2).

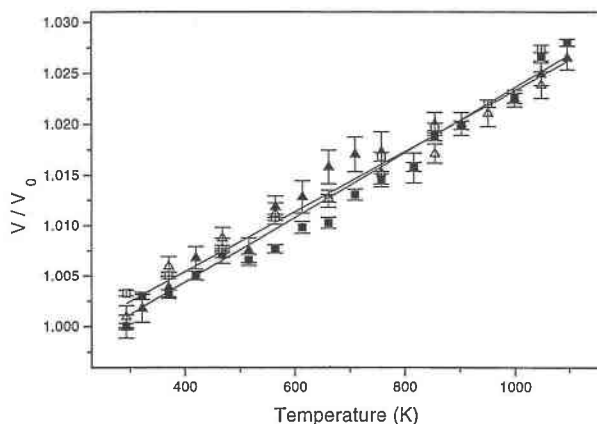


FIGURE 2. Comparison of the unit-cell volumes (shown as V/V_0) of MgSiO₃ orthoenstatite (squares) and MgSiO₃ clinoenstatite (triangles) up to 1094 K. Filled symbols represent data collected on increasing temperature; open symbols represent those collected on cooling.

TABLE 3. Unit-cell parameters for FeSiO₃ orthopyroxene constrained to orthorhombic symmetry

T (K)	a (Å)	b (Å)	c (Å)	Volume (Å ³)
293	18.392(10)	9.079(5)	5.236(3)	874.34(53)
322	18.393(9)	9.074(5)	5.246(5)	875.44(53)
370	18.403(7)	9.084(4)	5.251(2)	877.87(48)
419	18.428(11)	9.090(4)	5.251(2)	879.64(55)
467	18.427(8)	9.086(5)	5.253(2)	879.46(51)
515	18.446(6)	9.102(4)	5.239(2)	879.57(46)
563	18.444(11)	9.101(5)	5.263(3)	883.44(59)
612	18.466(9)	9.117(4)	5.252(2)	884.20(52)
660	18.490(10)	9.098(4)	5.261(2)	884.96(50)
708	18.448(9)	9.118(5)	5.259(2)	884.60(54)
756	18.465(11)	9.140(6)	5.253(2)	886.53(59)
805	18.471(9)	9.120(4)	5.264(2)	886.70(50)
853	18.495(16)	9.112(5)	5.275(3)	889.04(76)
901	18.516(11)	9.108(6)	5.274(4)	889.36(70)
853*	18.480(17)	9.109(5)	5.270(3)	887.15(78)
756*	18.488(10)	9.111(6)	5.262(3)	886.37(60)
660*	18.464(18)	9.097(6)	5.261(3)	883.65(79)
563*	18.439(16)	9.127(7)	5.246(2)	882.83(79)
467*	18.455(10)	9.099(5)	5.240(4)	879.77(73)
370*	18.376(10)	9.100(5)	5.236(3)	875.50(68)
293*	18.365(20)	9.084(9)	5.239(4)	874.05(93)

* Collected on temperature decrease, the remaining on initial heating.

TABLE 4. Unit-cell parameters for FeSiO₃ clinopyroxene constrained to monoclinic symmetry

T (K)	a (Å)	b (Å)	c (Å)	β (°)	Volume (Å ³)
293	9.721(6)	9.076(4)	5.227(5)	108.53(5)	437.26(63)
322	9.705(5)	9.082(7)	5.234(3)	108.49(3)	437.47(43)
370	9.714(5)	9.078(5)	5.234(4)	108.44(4)	437.89(47)
419	9.710(6)	9.103(5)	5.246(2)	108.58(4)	439.51(45)
467	9.709(5)	9.111(6)	5.243(3)	108.39(3)	440.07(48)
515	9.717(6)	9.086(5)	5.250(3)	108.48(4)	439.61(51)
563	9.713(5)	9.115(4)	5.256(2)	108.58(3)	440.54(36)
612	9.710(6)	9.105(4)	5.257(3)	108.63(4)	440.42(53)
660	9.728(7)	9.095(5)	5.254(3)	108.51(4)	440.82(59)
708	9.728(5)	9.108(3)	5.248(3)	108.56(3)	440.80(42)
756	9.740(8)	9.118(6)	5.253(4)	108.62(6)	442.07(69)
805	9.738(8)	9.114(5)	5.261(5)	108.74(6)	442.20(76)
853	9.706(7)	9.131(6)	5.262(4)	108.63(6)	441.87(56)
901	9.728(8)	9.124(6)	5.261(5)	108.16(6)	443.63(70)
853*	9.734(10)	9.128(5)	5.257(5)	108.66(5)	442.56(82)
756*	9.732(7)	9.119(5)	5.250(3)	108.59(5)	441.60(62)
660*	9.743(11)	9.106(6)	5.252(4)	108.53(4)	441.81(78)
563*	9.723(9)	9.119(6)	5.241(6)	108.66(6)	440.20(88)
467*	9.732(10)	9.106(9)	5.235(7)	108.63(7)	439.57(93)
370*	9.715(10)	9.080(6)	5.227(5)	108.46(7)	437.36(99)
293*	9.705(15)	9.102(8)	5.226(10)	108.32(11)	438.17(1.58)

* Collected on temperature decrease, the remaining on initial heating.

The linear thermal expansion coefficients for the direction perpendicular (100) are identical to within one combined estimated standard deviation, with values of $8.0(0.5) \times 10^{-6} \text{ K}^{-1}$ for the orthopyroxene polymorph and $7.6(0.6) \times 10^{-6} \text{ K}^{-1}$ for the clinopyroxene (Table 5). However, it is interesting that the relative thermal expansivities of the *b* and *c* axes of the two polymorphs are very different. Whereas the *b* axis of the orthopyroxene structure expands somewhat slower than that of the clinopyroxene, the *c* axis of the orthopyroxene expands at almost double the rate of the clinopyroxene (Table 5). The relative magnitudes of linear thermal expansion coefficients are in the order $\alpha_b > \alpha_c > \alpha_a$ for the orthopyroxene and $\alpha_b > \alpha_{d_{100}} > \alpha_c$ for the clinopyroxene phase.

Finally, although there is some scatter in the data, there is evidence (Table 2) that the β angle of the MgSiO₃ clinopyroxene increases slowly with increasing temperature. This effect, however, is small, with the change in β over the $\sim 800 \text{ K}$ temperature range being approximately 0.15° .

FeSiO₃

The unit-cell data for the ortho and clino polymorphs of FeSiO₃ pyroxene determined up to 901 K are given in Tables 3 and 4, respectively. A combined plot of V/V_0 for ortho- and clinoferrosilite (Fig. 3) demonstrates that, unlike the MgSiO₃ pyroxenes, the orthorhombic polymorph of FeSiO₃ expands considerably more than the monoclinic one over this temperature range; their respective volume thermal expansion coefficients at 293 K are $27.5(1.3) \times 10^{-6}$ and $20.3(1.5) \times 10^{-6} \text{ K}^{-1}$.

Comparison of the magnitudes of their linear axial thermal expansion coefficients shows that at 293 K for orthoferrosilite they are in the order $\alpha_a \approx \alpha_c > \alpha_b$, and in the order $\alpha_c > \alpha_b > \alpha_{d_{100}}$ for clinoferrosilite. These are summarized in Table 5. Whereas both the *b* and *c* axes

of the two FeSiO₃ polymorphs expand at identical rates within the experimental uncertainties, expansion in the direction perpendicular to the (100) planes occurs almost four times more in the orthopyroxene phase (Tables 3, 4, and 5).

The β angle of clinoferrosilite increases by approximately 0.15° over the 600 K temperature range studied (Table 4), giving a rate of expansion some $\sim 30\%$ greater than that of MgSiO₃ clinoenstatite.

DISCUSSION

Volume thermal expansion

The most recent analysis of the high-temperature behavior of synthetic (Mg,Fe)SiO₃ orthopyroxenes of vari-

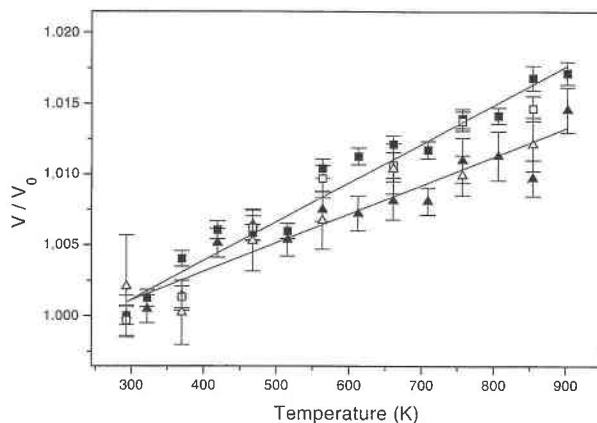


FIGURE 3. Comparison of the unit-cell volumes (shown as V/V_0) of FeSiO₃ orthoferrosilite (squares) and FeSiO₃ clinoferrosilite (triangles) up to 901 K. Filled symbols represent data collected on increasing temperature, open symbols represent those collected on cooling. Note the differing expansivities of the two polymorphs.

TABLE 5. Axial and volume thermal expansion coefficients for MgSiO₃ and FeSiO₃ pyroxenes

	Orthopyroxene		Clinopyroxene	
	α ($\times 10^{-6} \text{ K}^{-1}$)	<i>R</i>	α ($\times 10^{-6} \text{ K}^{-1}$)	<i>R</i>
	MgSiO₃			
<i>d</i> ₁₀₀	8.0(0.5)	0.949	7.6(0.6)	0.939
<i>b</i>	13.0(0.6)	0.974	16.6(0.5)	0.989
<i>c</i>	10.9(0.6)	0.961	5.2(0.7)	0.868
Volume	32.2(1.1)	0.987	29.9(1.1)	0.985
	FeSiO₃			
<i>d</i> ₁₀₀	10.4(1.0)	0.916	2.7(0.9)	0.601
<i>b</i>	6.8(1.5)	0.727	7.5(1.3)	0.800
<i>c</i>	10.1(1.4)	0.858	10.2(1.2)	0.889
Volume	27.5(1.3)	0.979	20.3(1.5)	0.952

Note: The "goodness-of-fit" of the data to the calculated value of α_v was measured by means of an *R* value, defined as $R = (V_{\text{obs}} - V_{\text{calc}})/(V_{\text{obs}})$.

ous compositions is that of Yang and Ghose (1994), who suggested that as the Fe content of the orthopyroxene is increased, so the volume thermal expansion coefficient at 293 K increases. Following their own high-temperature experiments, Sueno et al. (1976) compared their value of the volume thermal expansion coefficient of FeSiO₃ orthopyroxene with that of previous determinations and proposed that an entirely opposite trend may apply; this observation is supported by similar comparisons with previous thermal expansion data for a variety of other minerals (Cameron et al. 1973). Our data reinforce this earlier conclusion, with α_v increasing from $27.5(1.3) \times 10^{-6}$ to $32.2(1.1) \times 10^{-6} \text{ K}^{-1}$ as the composition changes from FeSiO₃ to MgSiO₃. The value of the thermal expansion coefficient, α_v , for FeSiO₃ orthoferrosilite is identical to that of Yang and Ghose (1994) within one combined estimated standard deviation, but some 25% lower than those of earlier workers (Table 6; Smyth 1973; Sueno et al. 1976).

A wider range of data is available for the α_v values of Mg-rich orthopyroxenes, from $20.8 \times 10^{-6} \text{ K}^{-1}$ (Dietrich and Arndt 1982) to $47.7 \times 10^{-6} \text{ K}^{-1}$ (Frisillo and Buljan

1972); however, this latter value is unusually high, with the majority of the data falling in the range $20.8 \times 10^{-6} \text{ K}^{-1}$ (Dietrich and Arndt 1982) to $36 \times 10^{-6} \text{ K}^{-1}$ (Sarver and Hummel 1962). The value of $32.2(1.1) \times 10^{-6} \text{ K}^{-1}$ calculated from this study is consistent therefore with the range of previously published values, although somewhat larger than most (Table 6).

Relatively few data are available in the literature concerning the thermal expansivity of (Mg,Fe)SiO₃ clinopyroxenes; however, the value of α_v at ambient temperature obtained from this study for the Mg end-member [namely, $29.9(1.1) \times 10^{-6} \text{ K}^{-1}$] is identical within one combined estimated standard deviation to that obtained by Pannhorst [1984; with $\alpha_v = 33.3(1.9) \times 10^{-6} \text{ K}^{-1}$], and lower than the value determined by Sarver and Hummel (1962; Table 6). The value of α_v at 293 K calculated for FeSiO₃ clinopyroxene from the data in Table 4 is $20.3(1.5) \times 10^{-6} \text{ K}^{-1}$; this is considerably lower than the values calculated for FeSiO₃ clinopyroxenes containing some 15–30 mol% Ca or Mg [Ohashi (1973) and Smyth (1974), respectively; Table 6]. No previous data exist for the volume thermal expansion coefficient of pure synthetic FeSiO₃ clinoferrosilite.

Assuming that there is a continuous change in behavior of (Mg,Fe)SiO₃ pyroxenes across the solid-solution join, the data in this present study indicate that all such Ca-poor orthopyroxenes have higher volume thermal expansion coefficients than the corresponding clinopyroxenes, irrespective of the relative Fe content of the sample. This is consistent with the data of Smyth (1973, 1974) for ortho- and clinopyroxene of intermediate composition Ca_{0.015}Mg_{0.305}Fe_{0.68}SiO₃ (Table 6). It is possible, however, that as the sample becomes increasingly Mg-rich, this effect becomes less pronounced, so that at the MgSiO₃ end-member composition the difference between the two values of α_v is only slightly greater than the experimental uncertainties. This is consistent with the data of Skinner (1966), who quotes, without uncertainties, values of 24×10^{-6} and $22 \times 10^{-6} \text{ K}^{-1}$, respectively, for the volume

TABLE 6. Comparison of axial and volume thermal expansion coefficients of (Mg,Fe)SiO₃ pyroxenes

Composition	Reference	<i>d</i> ₁₀₀	<i>b</i>	<i>c</i>	<i>V</i>
MgSiO ₃ opx	Sarver and Hummel (1962)	—	—	—	36
MgSiO ₃ opx	Skinner (1966)	—	—	—	24
MgSiO ₃ opx	Frisillo and Buljan (1972)	16.4	14.5	16.8	47.7
Mg _{0.95} Fe _{0.15} SiO ₃ opx	Dietrich and Arndt (1982)	—	—	—	20.8
MgSiO ₃ opx	Yang and Ghose (1994)	5.5	9.6	8.2	23.5
MgSiO ₃ opx	This study	8.0(0.5)	13.0(0.6)	10.9(0.6)	32.2(1.1)
Ca _{0.015} Mg _{0.305} Fe _{0.68} SiO ₃ opx	Smyth (1973)	13.5	14.5	15.4	43.8
FeSiO ₃ opx	Sueno et al. (1976)	11.2	10.9	16.8	39.3
FeSiO ₃ opx	Yang and Ghose (1994)	6.7	13.9	6.1	29.0
FeSiO ₃ opx	This study	10.4(1.0)	6.8(1.5)	10.1(1.4)	27.5(1.3)
MgSiO ₃ cpx	Sarver and Hummel (1962)	—	—	—	40.5
MgSiO ₃ cpx	Skinner (1966)	—	—	—	22
Mg _{0.95} Fe _{0.05} SiO ₃ cpx	Pannhorst (1984)	8.2	13.4	11.5	33.3
MgSiO ₃ cpx	This study	7.6(0.6)	16.6(0.5)	5.2(0.7)	29.9(1.1)
Ca _{0.15} Fe _{0.85} SiO ₃ cpx	Ohashi (1973)	8.9	13.3	15.2	37.6
Ca _{0.015} Mg _{0.305} Fe _{0.68} SiO ₃ cpx	Smyth (1974)	8.3	10.4	13.8	32.7
FeSiO ₃ opx	This study	2.7(0.9)	7.5(1.3)	10.2(1.2)	20.3(1.5)

Note: Expansion coefficients given as $\alpha_v \times 10^{-6} \text{ K}^{-1}$.

thermal expansion coefficients of MgSiO_3 , ortho- and clinoenstatite.

Linear thermal expansion

The order of axial thermal expansion coefficients determined from this study for MgSiO_3 , orthoenstatite (Table 5) are $\alpha_b > \alpha_a > \alpha_c$. This sequence is identical to that qualitatively determined by Dietrich and Arndt (1982), and the absolute values of the axial thermal expansion coefficients are within approximately two combined estimated standard deviations of those of Yang and Ghose (1994; Table 6). The available literature disagrees about the relative magnitudes of the axial thermal expansion coefficients of FeSiO_3 , orthoferrosilite (Table 6). However, the majority of these data (e.g., Smyth 1973; Yang and Ghose 1994) indicate that the rates of expansion of the a and c directions are approximately equal. Only the data of Sueno et al. (1976) support our data showing the b direction as having the lowest value of α_b . In the absence of experimental uncertainties in these published data, however, it is difficult to make further comparisons.

This study has shown that the relative axial thermal expansion coefficients of MgSiO_3 , clinoenstatite are in the order $\alpha_b > \alpha_{d_{100}} > \alpha_c$. If it is considered that within two combined estimated standard deviations the thermal expansivities in the directions perpendicular to either (100) or (001) planes are equal, then these data agree with those of Pannhorst (1984; Table 6). The data presented in Table 4 for the relative axial thermal expansion coefficients of FeSiO_3 , clinoferrosilite are identical to those of Ohashi (1973) and Smyth (1974), although it is interesting to note that our value for $\alpha_{d_{100}}$ is some three times less than either of those calculated by these authors for their Ca- or Mg-containing clinoferrosilites.

The β angle

The data collected from both MgSiO_3 and FeSiO_3 , clinopyroxenes has shown that β increases as the temperature increases. However, comparison with the data of Pannhorst (1984) and Smyth (1974) shows that the increase in β in the present data (Tables 2 and 4) is considerably less than that observed over a similar temperature range for their MgSiO_3 and $\text{Ca}_{0.015}\text{Mg}_{0.305}\text{Fe}_{0.68}\text{SiO}_3$ clinopyroxenes, respectively.

Comparisons with compressibilities data

Recent compressibility data collected from synthetic MgSiO_3 and FeSiO_3 , ortho- and clinopyroxenes (Hugh-Jones and Angel 1994; Hugh-Jones 1995) show that the initial compressibility of orthopyroxene is significantly greater than that of clinopyroxene of the same composition and that the compressibility of Fe-rich pyroxenes is marginally greater than that of Mg-rich pyroxenes. The reasons for this slightly increased compressibility of the Fe-rich orthopyroxenes may be explained in terms of the structural differences between Mg- and Fe-containing pyroxenes (discussed below). The data of Hugh-Jones and Angel (1996) and Hugh-Jones (1995) also show that all

(Mg,Fe) SiO_3 pyroxenes (whether ortho or clino) have relative linear axial compressibilities in the order $\beta_b > \beta_c > \beta_a$; in contrast, the order of axial thermal expansivities of the pyroxenes depends on both their compositions and structures (Table 5).

Structural aspects

Pyroxenes consist of layers of SiO_4 tetrahedra joined by bridging O atoms to form chains running parallel to [001]. Between these tetrahedral layers are layers of octahedrally coordinated cations, contained in two structurally distinct sites, known as M1 and M2 sites. The M1 site is smaller and less distorted than the M2 site. Both ortho- and clinopyroxenes (with space groups $Pbca$ and $P2_1/c$, respectively) have two crystallographically distinct tetrahedral chains contained within the tetrahedral layer: The "A" chain is straighter with somewhat smaller tetrahedra, whereas the more kinked chain with larger tetrahedra is known as the "B" chain. The difference between ortho- and clinopyroxenes lies in the relative rotation of the tetrahedral "A" chain compared to the cation octahedra in the layer below: Orthopyroxenes contain O-rotated "A" chains, whereas clinopyroxenes contain S-rotated "A" chains (following the notation of Thompson 1970). Both structures have O-rotated "B" chains.

Because Fe^{2+} is significantly larger than Mg, the M1 and M2 sites of both the FeSiO_3 polymorphs are correspondingly larger and more distorted than those in MgSiO_3 pyroxenes (Domeneghetti and Steffen 1992; Hugh-Jones 1995). They are also more compressible than the Mg-containing sites, suggesting that, because the volumes of the SiO_4 tetrahedra in all pyroxenes are effectively unchanged during heating (e.g., Smyth 1974; Yang and Ghose 1995) or with initial compression (Hugh-Jones and Angel 1994), the FeSiO_3 pyroxene structure as a whole should be more compressible than the MgSiO_3 one (as observed by Hugh-Jones 1995). Mg-rich pyroxenes are therefore initially more "compact" than Fe^{2+} -rich ones because of their smaller cation sites, generally giving them more scope for expansion at high temperatures and correspondingly less during compression; the data in Table 5 confirm that both ortho and clino MgSiO_3 pyroxenes have higher volume thermal expansion coefficients than FeSiO_3 pyroxenes.

The orthopyroxene structure for both end-member compositions of the (Mg,Fe) SiO_3 solid solution is initially more compressible than that of clinopyroxene (Hugh-Jones 1995); the data in Table 5 show that the same orthopyroxenes also expand more quickly than the clinopyroxenes. Orthopyroxene is thus the more flexible structure, allowing easier compression and expansion of the structure than clinopyroxene, irrespective of the relative sizes of the Mg- or Fe-containing cation sites.

It is easy to understand, when considering the axial compressibilities of the pyroxene polymorphs, that the most compressible direction is that which contains the maximum amount of "free space" at ambient conditions,

namely, the *b* direction. The next most compressible direction in all (Mg,Fe)SiO₃ ortho- and clinopyroxene polymorphs is the *c* direction (Hugh-Jones 1995), which is parallel to the tetrahedral chains within the structure and therefore that most affected by the kinking of the chains under pressure. It was expected that the response of these pyroxenes to increasing temperature would reflect this compressional behavior, with the order of axial expansion being identical to the order of linear compressibilities, i.e., $\beta_b > \beta_c > \beta_a$. This trend can indeed be seen in the data for MgSiO₃ orthopyroxene (Table 5).

However, the changing order of axial expansivities for (Mg,Fe)SiO₃ ortho- and clinopyroxenes (Table 6) suggests that no simple rule is followed on heating like that observed during compression. Structural data (Hugh-Jones et al. 1994; Ohashi 1984) indicate that for ortho- and clinopyroxenes of each end-member composition, the sizes and distortions of both octahedral and tetrahedral cation sites are identical within the experimental uncertainties. Thus the differences in relative axial expansivities are probably due to the complex interplay of internal strains within the structures arising from the relative expansion of the M1 and M2 polyhedra (the magnitude depending on the cation contained within the sites; e.g., Sueno et al. 1976; Smyth 1973; Yang and Ghose 1995) and the amount of extension of the silicate chains with increasing temperature (measured by the O3-O3-O3 chain extension angle, and generally between 0.5° and 1° per 100 K temperature rise; e.g., Sueno et al. 1976; Smyth 1973; Smyth 1974; Pannhorst 1984); silicate tetrahedra tend to show slight negative thermal expansion over the temperature ranges studied. It is beyond the scope of this paper (having collected no further structural data for the MgSiO₃ and FeSiO₃ pyroxenes at high temperatures) to suggest reasons for these differences.

Thermodynamic implications for MgSiO₃

Simple thermodynamic calculations, based on the solution of the equation $\Delta G = \Delta H - T\Delta S + P\Delta V = 0$, show that the crucial factor determining the nature and magnitude of the slope of the phase boundary between MgSiO₃ ortho- and clinoenstatite is the relative thermal expansion of the two phases. Indeed, this was the motivation for undertaking this study. A preliminary calculation, using data for the entropy and enthalpy of the two phases calculated from their respective heat capacities (Robie et al. 1978; Thiéblot 1992), compressibility data from Angel and Hugh-Jones (1994), and various combinations of the previously published data for the thermal expansion coefficients of the two phases, gave an extremely poorly constrained phase boundary with a slope ranging from a highly negative value of dP/dT to a highly positive one.

However, by using the thermal expansion data presented in Table 5, a very well constrained phase boundary was obtained; this is shown in Figure 4, superimposed onto the phase diagram for MgSiO₃ pyroxenes (Angel and Hugh-Jones 1994). The fit between the two is excellent

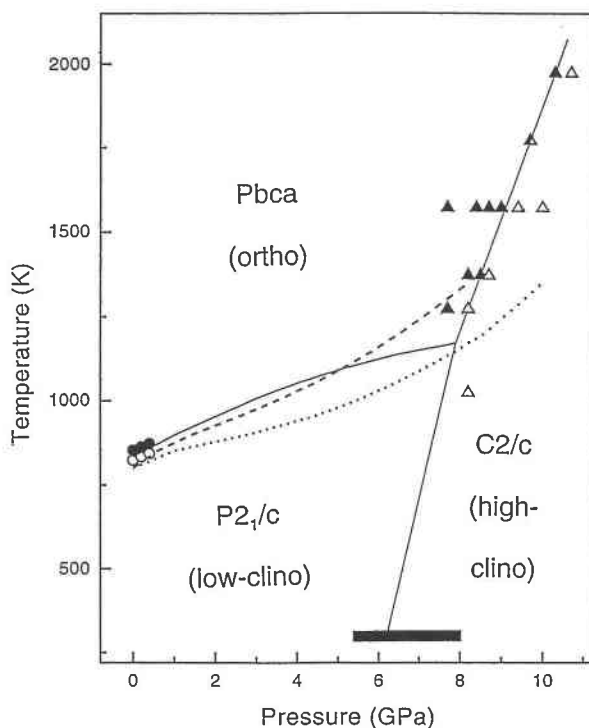


FIGURE 4. Phase diagram of MgSiO₃ pyroxene (after Angel and Hugh-Jones, 1994), showing the position (dashed line) of the newly calculated phase boundary between the ortho- and clinoenstatite polymorphs. Further calculations, assuming the thermal expansion coefficients of the two phases to be identical (see text), yield a phase boundary shown by the dotted line. The triangles represent the reversal data of Pacalo and Gasparik (1990), circles the data of Grover (1972), and the box represents the reversal bracket on the ortho- to high-pressure clinoenstatite transition determined at ambient temperature by Angel et al. (1992).

at pressures below ~6 GPa; the new boundary is also consistent with the limited low-pressure reversal data of Grover (1972). At pressures between 6 GPa and the triple point (~7.9 GPa), there appears to be some deviation, but too few experimental data exist at these pressures and temperatures to dispute its validity.

The above calculation assumed no change of either bulk moduli with temperature; however, no significant change in the position of the phase boundary between the two phases in *P-T* space was observed upon the inclusion of a term for dK/dT for the two phases (e.g., Zhao et al. (1995), assuming identical values of dK/dT for both ortho- and clinopyroxene polymorphs). If, on the other hand, the volume thermal expansion coefficients of the two phases are considered to be identical [and constrained to be either 32.2×10^{-6} or 29.9×10^{-6} K⁻¹ (Table 5)], the boundary is shifted to slightly lower temperatures (Fig. 4), although it is still consistent with the reversal data of Grover (1972). In conclusion, it is therefore likely that the small difference in volume thermal expansion coefficients observed in this study between MgSiO₃ or-

tho- and clinopyroxene is significant in determining the precise nature of the phase boundary between them.

Finally, it is unfortunate to note that there are insufficient thermodynamic data available for a similar calculation to be performed for the FeSiO_3 polymorphs.

ACKNOWLEDGMENTS

I would like to thank A. Graeme-Barber for her advice on the computer techniques available for refinement of the unit-cell parameters and for making her high-temperature unit-cell data for quartz available for comparison with ours. I would also like to thank B. Cullum and T. Abraham for their assistance during the synthesis and high-temperature X-ray experiments, respectively, and R.J. Angel and S.A.T. Redfern for their constructive comments on the initial draft of this manuscript.

REFERENCES CITED

- Angel, R.J. and Hugh-Jones, D.A. (1994) Equations of state and thermodynamic properties of enstatite pyroxenes. *Journal of Geophysical Research*, 99, 19777–19783.
- Angel, R.J., Woodland, A.B., and Hugh-Jones, D.A. (1994) Phase equilibria of FeSiO_3 pyroxenes (abstract) IMA Meeting, Pisa, p.13.
- Cameron, M., Sueno, S., Prewitt, C.T. and Papike, J.J. (1973) High-temperature crystal chemistry of acmite, diopside, hedenbergite, jadeite, spodumene, and ureyite. *American Mineralogist*, 58, 594–618.
- Dietrich, P. and Arndt, J. (1982) Effects of pressure and temperature on the physical behaviour of mantle-relevant olivine, orthopyroxene and garnet: I. Compressibility, thermal properties and macroscopic Grüneisen parameters. In W. Schreyer, Ed., *High-Pressure Researches in Geosciences*, p. 293–306. Schweizerbart'sche Verlagsbuchhandlung, Stuttgart.
- Domeneghetti, C.M. and Steffen, G. (1992) M1, M2 site populations and distortion parameters in synthetic Mg-Fe orthopyroxenes from Mössbauer spectra and X-ray structure refinements. *Physics and Chemistry of Minerals*, 19, 298–306.
- Frisillo, L.A. and Buljan, S.T. (1972) Linear thermal expansion coefficients of orthopyroxene to 1000 °C. *Journal of Geophysical Research*, 77, 7115–7117.
- Gasparik, T. (1990) A thermodynamic model for the enstatite-diopside join. *American Mineralogist*, 75, 1080–1091.
- Grover, J. (1972) The stability of low-clinoenstatite in the system $\text{Mg}_2\text{Si}_2\text{O}_7\text{-CaMgSi}_2\text{O}_6$ (abstract). *Eos, Transactions of the American Geophysical Union*, 53, 539.
- Hugh-Jones, D.A. and Angel, R.J. (1994) A compressional study of MgSiO_3 orthoenstatite up to 8.5 GPa. *American Mineralogist*, 79, 405–410.
- Hugh-Jones, D.A., Woodland, A.B., and Angel, R.J. (1994) The structure of high-pressure *C2/c* ferrosilite and crystal chemistry of high-pressure *C2/c* pyroxenes. *American Mineralogist*, 79, 1032–1041.
- Hugh-Jones, D.A. (1995) High pressure behaviour of pyroxenes. PhD thesis, University College, London.
- Hugh-Jones, D.A. and Angel, R.J. (1997) Effect of Ca^{2+} and Fe^{2+} on the equation of state of MgSiO_3 orthopyroxene. *Journal of Geophysical Research*, in press.
- Ohashi, Y. (1973) High-temperature structural crystallography of synthetic clinopyroxene (Ca,Fe) SiO_3 . Ph.D. thesis, Harvard University, Cambridge, Massachusetts.
- (1984) Polysynthetically-twinned structures of enstatite and wolastonite. *Physics and Chemistry of Minerals*, 10, 217–229.
- Pacalo, R.E.G. and Gasparik, T. (1990) Reversals of the orthoenstatite-clinoenstatite transition at high pressures and temperatures. *Journal of Geophysical Research*, 95, 15853–15858.
- Pannhorst, W. (1984) High temperature crystal structure refinements of low-clinoenstatite up to 700 °C. *Neues Jahrbuch für Mineralogie Abhandlungen*, 150, 219–228.
- Perotta, A.J. and Stephenson, D.A. (1965) Clinoenstatite: high-low inversion. *Science*, 148, 1090–1091.
- Prewitt, C.T., Brown, G.E., and Papike, J.J. (1971) Apollo 12 clinopyroxenes: High temperature X-ray diffraction studies. *Proceedings of the Lunar Science Conference*, 2, 59–68.
- Robie, R.A., Hemingway, B.S., and Fisher, J.R. (1978) Thermodynamic properties of minerals and related substances at 298.15 K and 1 bar (10^5 pascals) pressure and at higher temperatures. *U.S. Geological Survey Bulletin*, 1452, p. 456.
- Salje, E.K.H., Graeme-Barber, A., and Carpenter, M.A. (1993) Lattice parameters, spontaneous strain and phase transitions in $\text{Pb}_3(\text{PO}_4)_2$. *Acta Crystallographica*, B49, 387–392.
- Sarver, J.F. and Hummel, F.A. (1962) Stability relations of magnesium metasilicate polymorphs. *Journal of the American Ceramic Society*, 45, 152–157.
- Skinner, B.J. (1966) Thermal expansion. In S.P. Clark Jr., Ed., *Handbook of Physical Constants*, p. 75–95. Geological Society of America, Boulder, Colorado.
- Sueno, S., Cameron, M., and Prewitt, C.T. (1976) Orthoferrosilite: High-temperature crystal chemistry. *American Mineralogist*, 61, 38–53.
- Smith, J.V. (1969) Crystal structure and stability of the MgSiO_3 polymorphs; physical properties and phase relations of Mg,Fe pyroxenes. *Mineralogical Society of America Special Paper*, 2, 3–29.
- Smyth, J.R. (1973) An orthopyroxene structure up to 850 °C. *American Mineralogist*, 58, 636–648.
- (1974) The high-temperature crystal chemistry of clinohypersthene. *American Mineralogist*, 59, 1069–1082.
- Thiéblot, L. (1992) Etude des propriétés thermodynamiques de l'ortho-enstatite et du grossulaire. *Rapport de D.E.A. de géochimie fondamentale, Université Paris 7*.
- Thompson, J.B., Jr. (1970) Geometrical possibilities for amphibole structures: model biopyriboles. *American Mineralogist*, 55, 292–293.
- Yang, H. and Ghose, S. (1994) Thermal expansion, Debye temperature and Grüneisen parameter of synthetic (Fe,Mg) SiO_3 orthopyroxenes. *Physics and Chemistry of Minerals*, 20, 575–586.
- (1995) A transitional structural state and anomalous Fe-Mg order-disorder in Mg-rich orthopyroxene ($\text{Mg}_{0.75}\text{Fe}_{0.25}$) Si_2O_6 . *American Mineralogist*, 80, 9–21.
- Zhao, Y., Schiferl, D., and Shankland, T.J. (1995) A high P-T single-crystal X-ray diffraction study of thermoelasticity of MgSiO_3 orthoenstatite. *Physics and Chemistry of Minerals*, 22, 393–398.

MANUSCRIPT RECEIVED AUGUST 16, 1996

MANUSCRIPT ACCEPTED MARCH 7, 1997